CA Models of Myxobacteria Swarming

Yilin Wu[1], Nan Chen[1], Matthew Rissler[1], Yi Jiang[2], Dale Kaiser[3], and Mark Alber[1]

[1] Department of Mathematics and Center for the Study of Biocomplexity,
University of Notre Dame, Notre Dame, IN 46556-5670
{Yilin.Wu.34, NAN.Chen.93, Matthew.Rissler.4, malber}@nd.edu
[2] Theoretical Division, Los Alamos National Laboratory, Los Alamos, NM 87545
jiang@lanl.gov
[3] Department of Biochemistry, Stanford University, Stanford, CA 94305
kaiser@pmgm2.stanford.edu

Abstract. We develop two models for Myxobacteria swarming, a modified Lattice Gas Cellular Automata (LGCA) model and an off-lattice CA model. In the LGCA model each cell is represented by one node for the center of mass and an extended rod-shaped cell profile. Cells check the surrounding area and choose in which direction to move based on the local interactions. Using this model, we obtained a density vs. expansion rate curve with the shape similar to the experimental curve for the wild type Myxobacteria. In the off-lattice model, each cell is represented by a string of nodes. Cells can bend and move freely in the two-dimensional space. We use a phenomenological algorithm to determine the moving direction of cells guided by slime trail; the model allows for cell bending and alignment during collisions. In the swarming simulations for A+S- Myxobacteria, we demonstrate the formation of peninsula structures, in agreement with experiments.

Keywords: probabilistic cellular automata, lattice and off-lattice models, bacteria swarming, slime guidance, pattern formation.

1 Introduction

Myxobacteria (Myxococcus xanthus) are social bacteria that live in the soil; they exhibit complex multi-cellular behavior and provide many useful insights to multicellular morphogenesis. They are rod shaped with an aspect ratio of roughly 10:1. When growing on a solid medium with sufficient nutrient, Myxobacterial cells grow as a swarm that spreads outwards from the origin, forming rafts and group of cells that project from the edge of the swarm (peninsula structures) [1] (see Figure 1). When nutrient is depleted, the starved Myxobacteria stop growing and build fruiting bodies [2, 3].

Myxobacteria moves by gliding on surfaces, it cannot swim in liquid [4]. It has two types of motility, S(social)-motility and A(adventurous)-motility that are driven by different engines. S-motility is due to pilus extension from the front end of the cell, attachment of the pilus tip to a group of cells ahead, and pilus retraction, drawing the cell up to the leading group [4]. A-motility is due to secretion of polysaccharide slime from the rear of the cell. The hydration-driven swelling of the slime gel is suggested

S. El Yacoubi, B. Chopard, and S. Bandini (Eds.): ACRI 2006, LNCS 4173, pp. 192 – 203, 2006.

to generate the pro-pulsive force for A-motility [5]. A+S- mutants of Myxobacteria have only A-motility but no S-motility , while those with S-motility but no A-motility are called A-S+ mutants [1]. Individual Myxobacteria cells reverse their gliding direction roughly once every 10 min, and the mglA mutants which are unable to reverse normally are unable to swarm [2, 4, 12].

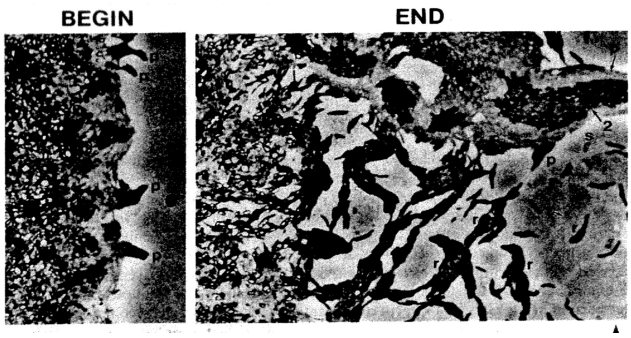

Fig. 1. The swarming patterns of wild-type A+S+ Myxobacteria (Picture taken from [1], by Kaiser, D. and C. Crosby (1983)). On the upper-left part of the END picture, a large peninsula projected outwards from the colony edge. There were also smaller peninsulas and rafts of cells.

Isolated cells move along their long axis and may bend slightly [1, 2]. When a cell is less than a pilus length from other cells, S-motility can be active because the pili can reach groups of other cells that are ahead [2]. As the cells move, they leave a slime trail behind which pushes the cells forward (A-motility). Experimental observations showed that when cells meet a slime trail, they tend to turn at the acute angles to follow the trail [8].

Swarming of Myxobacteria has been modeled using a continuous model with partial differential equations (PDE) [9], which treats the radial swarming pattern expansion as a one-dimensional problem and assumes a rate at which peninsulas merge.

In this paper, we first present a modified two-dimensional LGCA model, and investigate the expansion rate as well as the peninsula formation in wild type Myxobacteria during swarming. We then present an off-lattice model, which is the first computational model based on slime guidance for cells and motility engine reversal. We describe preliminary simulations for the swarming of A+S- Myxobacteria, which successfully reproduce the peninsula pattern.

2 Lattice Gas Cellular Automata (LGCA) Model

2.1 Description

Unlike classical LGCA [10], in our model each cell is not simply a point particle, it has an extended domain (profile) that encompasses several lattice sites. (Notice that

the extended profiles have been used previously, amongst others, for modeling collective cell movement in *Dictyostelium discoideum* [11].) Each cell is defined by the position of its center of mass on the two dimensional hexagonal lattice, direction of movement (when it is moving), its length and the extent of its bending. From these five state variables we determine the extended domain (profile) of the cell. Cell direction is updated using a Monte Carlo algorithm.

Three representative cells and the surrounding search area of one of the cells are displayed in Figure 2. Each cell has a length of 7 sites and a width of 1 site. The sites of the cell are indexed from the back of the cell to the front of the cell. The center of mass of the cell is always at half of the cell length. The dark grey spot is the center of mass, and the black ones are the rest of the body of the cell. The shaded spots are to show the search area for S-motility. The length of the cell changes as the cell absorbs a diffusing nutrient until it reaches a maximum value. Then the cell divides into two equal halfs.

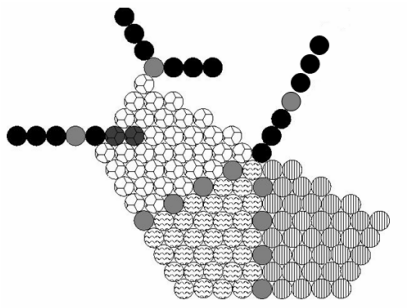

Fig. 2. Three representative cells and the surrounding search area of one of the cells. The three cells are represented by the groups of black circles with the center of mass node in light gray. The three areas below the cell on the right represent the search areas for the S-motility algorithm. The four sites that are shaded dark between two searching areas belong to both areas.

Cells choose which direction to turn at each time step based on three components, slime, S-motility, and physical contact with other cells. Cells tend to align with the direction of previous cells that have passed and deposited slime. S-motility is pili driven, and we model it by favoring cells to be pulled towards areas of higher local cell density. Physical contact accounts for side-to-side alignment due to adhesion, deflections by collisions with other cells, and physical obstacles to turning caused by nearby cells.

We assign a weight, α_i to each effect listed above. For each cell we collect data pertaining each of them, $f_i^{\,j}(x)$, where x is the current system state and $f_i^{\,j}$ is the function describing the strength of an effect in the jth direction. The detailed explanations for $f_i^{\,j}$ are listed in Table 1.

Table 1. The local information collected to model each effect for determining cell turning and bending

	Effect modeled	*Data collected*
f_1	A- motility	The amount of slime deposited on the three lines passing through the center of mass of the cell.
f_2	S- motility	The number of occupied sites in each of the three regions of Illustration 1.
f_3	Cell-Cell alignment	The number of sites that will contain a parallel cell beside this cell if it turns in this direction.
f_4	Collisions	The number of cells one lattice site in front of the current cell that are not aligned with this cell
f_5	Crowding	The negative of the number of occupied lattice sites that are in the triangle formed between the current cell and the cell if it turns this direction.

The cell is only allowed to bend 60° to the left or right. After these function values are collected we assign each of the possible outcomes a probability $P(j)$ calculated as follows:

$$P(j) = \frac{\sum_{i=1}^{5} e^{\frac{\alpha_i f_i^j(x)}{\beta}}}{Z}, \text{ where } Z = \sum_{j=1}^{3}\sum_{i=1}^{5} e^{\frac{\alpha_i f_i^j(x)}{\beta}}$$

This choice of probability function provides a good separation of similar states, with β corresponding to the amount of separation. The new direction for the cell is determined by this probability. To model motility mutants, A^+S^- and A^-S^+, we set $\alpha_2 = 0$ and $\alpha_1 = 0$ respectively.

A cell moves one step forward and straightens as long as this does not cause it to overrun another cell, otherwise it stalls, and stays bent. All cells turn or bend simultaneously, so collisions that involve two cells moving into an unoccupied space are not prevented. After that all cells move simultaneously. After movement, cells can grow, deposit slime, or reverse with a preset period. The time step and lattice spacing are matched to produce the appropriate velocity for the motilities of the cells.

2.2 Simulation Results

We simulated circular colonies of A+S+ wild type Myxobacteria of initial radius 60 μm and varying initial densities. We first calculate the radial distribution function of cell density for the entire colony. Then define the edge of the colony by a cell density threshold of the distribution. The rate of expansion was then calculated from the linear fit for the distance to the colony edge versus time.

The expansion rates from simulations were plotted against the initial density of the colony, the plot was fit by this function:

$$f(x) = A + B\left(1 - \exp\left(\frac{x}{C}\right)\right)$$

where x is the initial density, as in [1]. From simulation data, a fit of A=-0.1±0, B=0.5±0.2, C=50±20 was found for wild-type cells. In the experiment with an initial radius of 1.5 mm [1], the fit of the same form for wild type cells was A=0.1, B=1.48, C=48±6, with A+B=1.58±0.06. While the length scale between the simulation and experiment differ by 3 orders of magnitude, the expansion rate was constant over two orders of magnitude for the simulation.

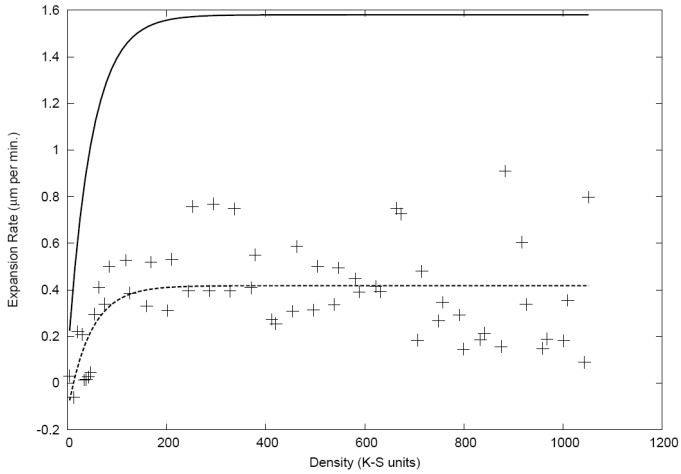

Fig. 3. Density (X-axis,) vs. Growth Rate (Y-axis,) curves for experiment (upper) and simulation (lower). The density is in Klett-Summerson unit [1], and the growth rate is in unit of microns per minute. The exes are simulation results.

Figure 4 shows the peninsulas that formed from an initial smooth colony edge. The peninsulas appear mostly in the areas of the initial circle of cells where the radius aligned with a direction of the lattice. This agrees with experimental observation that cells are initially aligned perpendicularly to the colony boundary.

Fig. 4. The initial condition and a representative snapshot of a myxobacteria colony after 300 time steps. The snapshot demonstrates peninsulas that curve and merge, as well as rafts of cells. Five peninsulas exist in this snapshot.

From our simulations, we find that the exponent, C, in the expansion function agrees with experimental measurements within error; we also observe the peninsulas forming. But the overall expansion rate is much lower than the experimental measurements. This is due to several artifacts in our model. The first is that peninsulas form mostly at the corners of a hexagon centered at the center of the colony, since this is the only point on the boundary where a direction normal to the boundary is allowed. If a cell attempts to leave the colony at another point, the local rules for S-motility turn it back into the colony, since pili are modeled to prefer areas of higher cell density. This S-motility effect also causes a negative expansion rate at low densities. Secondly, due to the rigidity of the cells, cells collide with each other and cannot easily free themselves from the current configurations. Therefore in the high density area in the initial colony, cells become entrapped and can not move. We overcome these difficulties by introducing an off-lattice model, which is described in the next section.

3 Off-Lattice Model

3.1 Modeling Individual Cell

To incorporate into the model the elastic properties of the Myxobacteria cell body as described in [12], we adopt an off-lattice cell representation to allow for more flexible cell shape and mechanical properties [13]. An individual cell's configuration is represented by a string of N nodes (Figure 5) which can occupy any positions in two-dimensional space. The first node is called the head-node, and the N-th node is called the end node. The vector pointing in the direction from the end-node to the head-node determines the cell's orientation. There are (N-1) segments of length r each between every two neighboring nodes. There are also (N-2) angles θ between every two neighboring segments. We define the Hamiltonian for an individual cell (see Figure 5) as follows:

$$H = E_{stretching} + E_{bending}$$

Stretching and bending energies are defined as a quadratic function of segment length r between nodes and the angles θ between two segments respectively, i.e. we approximate the cell body as having simple elastic stretching and bending energies:

$$E_{stretching} = \sum_{i=0}^{N-1} K_b (r_i - r_0)^2, \qquad E_{bending} = \sum_{i=0}^{N-2} K_\theta \theta_i^2$$

Here K_b and K_θ are parameters analogous to the spring constants in Hooke's Law; they determine the extent to which the segment lengths and angles can change in the presence of external forces, respectively. They are the same for all segments and angles. r_0 is the target length of the segment.

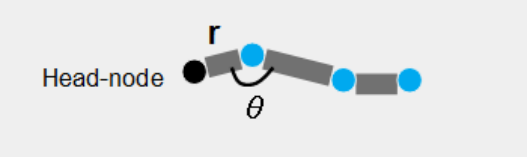

Fig. 5. A cell body of Myxobacteria is represented by N=4 nodes. The black solid dot is the head-node. The length to width ratio of the cell is 10:1.

The relative positions of nodes can change during the configuration updates in our algorithm, so the cell body is flexible.

The Monte Carlo approach is used for configuring the position of the nodes at every time step. We first move the head-node to a new position, denoting the magnitude of the displacement as Δx, and then repeat the following steps for a sufficient number of times (we choose this number as 2.5N): 1. Randomly choose a node within the same cell, for instance, node i, and move it in the direction from node i to node $(i-1)$ for a distance of Δx, with a small random fluctuation; 2. Calculate the energy change ΔE due to the relative position change of the nodes; 3. Use the Metropolis algorithm [14] to determine the acceptance probability for the positional change of a node:

$$P(\Delta E) = 1, \Delta E \le 0;$$

$$P(\Delta E) = e^{-\Delta E / kT}, \Delta E > 0$$

Here k is a Boltzmann constant; T is a parameter that characterizes the system's tendency to statistically fluctuate from the equilibrium. The cells in the model can bend elastically due to the random fluctuation during the updating of nodes configurations while keeping their lengths within certain range.

3.2 Modeling Cell Motion

In our off-lattice model, cells are allowed to move freely in any direction in the two-dimensional space. This is a significant improvement compared to the lattice models where cells move on a fixed lattice.

Biologically, wild type A+S+ Myxobacteria cells move by using pulling force from pili retraction at the head and pushing force from slime secretion at the end. We focus on the global motion of a large number of cells during swarming instead of studying details of motility mechanisms of an individual cell. Therefore, we model the cell's effective motion by using simplified assumption about the motion of a cell being led by the head. That is, the head of a cell pulls the whole cell body to move forward. We distinguish cells with different types of motility through a variable magnitude of the head velocity. In this preliminary model, we only include the A-motility and fix the magnitude of the head velocity at about 4 microns per minute.

In experiment, an isolated cell moves along the direction of its long axis and keeps roughly straight. When meeting a slime trail, cells tend to turn at the acute angles to follow the trail [8]. When cell density is high, as they are at the colony's edge at early

stage of Myxobacteria swarming, cells are packed layer by layer, and they can move on top of other cells. In this case, there will be a lot of intersecting slime trails and cells may not follow a particular slime trail. On the other hand, collisions between cells are more important than cell-slime interactions at high cell densities. For these reasons, we define a searching circle centered at the head node of each cell (Figure 6), and define a local slime field density *D(s)* for each cell as the total area covered by slime within the divided by the area of searching circle (Figure 6):

$$D(s) = \frac{\text{(area covered by slime)}}{\text{(area of searching circle)}}$$

We then let the cell follow a particular slime trail only if the slime field density is below a certain threshold. Because the width of a slime trail is close to cell-width, while the radius of searching circle is defined to be about half of a cell-length, then the slime field density for a searching circle with single slime trail will be:

$$\frac{2\cdot(\text{radius of searching circle})\cdot(\text{width of slime trail})}{\pi\cdot(\text{radius of searching circle})^2} \simeq \frac{4\cdot(\text{cell-width})}{\pi\cdot(\text{cell-length})}$$

A typical cell's width-to-length ratio is 1:10, so we choose the threshold of slime field density to be 0.2, which corresponds to only a few slime trails in the simulation domain.

Based on experimental observations of cell motion, we develop a phenomenological algorithm to determine the direction of head node velocity, which we call the head-sensing slime guidance algorithm (see Figure 6):

(1) Search the circlar area ahead of the cell for slime trail and calculate the local slime field density *D(s)*;
(2) If no slime trail is found, or if $D(s)>0.2$, choose the cell orientation as head velocity direction and go to step (6) (The cell's orientation is defined by the vector pointing in the direction from end to head). If $D(s)\leqslant 0.2$, go to next step;
(3) Approximate the direction of the slime trail as a line segment (from point A to B);
(4) Transform the coordinate of point A and B from XOY to the cell's local coordinate system (X'O'Y');
(5) If Y' of one point is less than that of the other one, for instance, Y'(A) < Y'(B), then choose the new direction as O'→B because cells tend to turn at the acute angles to follow slime trails; if the new direction opposes the cell direction and thus may reduce the cell length, choose the new direction as A→B. In the case of Y'(B) < Y'(A), simply change O'→B (or A→B) to be O'→A (or B→A).
(6) Tentatively advance the cell using the head velocity obtained through the above procedures. If it collides with another cell, choose the collided cell's orientation as the new head-velocity direction, so that cells can align with each other when collision happens.

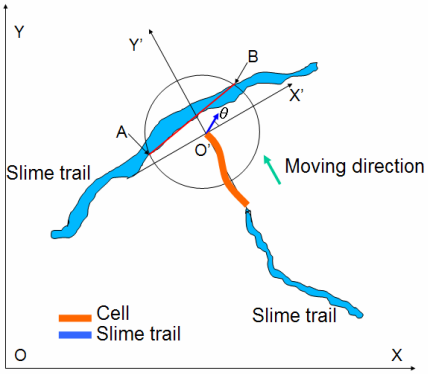

Fig. 6. A schematic description of head-sensing slime guidance for Myxobacteria cells. The orange lines represent a part of cell body, which meets with a slime trail. The head of the cell is defined as O' point, the origin of the cell's local coordinate system X'O'Y'. The cell orientation is along the direction of O'Y'. The cell will turn to a new direction at an angle θ with O'X' axis when it meets the slime trail.

In our simulation, cells move at most 0.8 micron every time step, so 5 simulation time steps correspond to one minute of real time. At each time step, we do the following for each cell in the order of numbering of cells: First, find out the moving direction for its head node by the head-sensing slime guidance algorithm. If no collision happens in the direction, move the head node for a distance of 0.8 microns; otherwise the cell stalls and waits until next time step for a new moving direction. Next, apply the Monte Carlo algorithm described in section 3.1 to re-configure the positions of the rest nodes. Besides, cells reverse polarity every 50 time steps. We also include cell divisions. Typically cells divide after more than 10 times reversals [6]. The division rate is set in such a way that the total number of cells approximately doubles after about 3 hours, which is the typical duoubling time of the swarming stage.

3.3 Simulation Results

We first run simulations to demonstrate the head-sensing slime guidance algorithm for cells. As shown in Figure 7(a-d), the cells could efficiently orient along slime trails. Initially 10 cells were randomly distributed in space. The black dots and lines represent slime (cells are not shown in the figure).

In swarming experiments, tens of thousands of cells form a solid wall at the edge of a circle with a radius of about 1.5 mm [1]. Due to the computation limit, we first look at a small curved section which is 167 microns in length and 17 microns in width. The length is about 1/60 of the perimeter of circle. Because the length of the section is much smaller than the radius of circle, the small section can be approximated as a rectangular area. We use a 1000×1000 square as the simulation domain as shown in Figure 8, and the rectangular area is indicated as "Initial Area of Cells". 1000 units of length are equivalent to 167 microns, so 6 units of length are equivalent to 1 micron. We distribute 1111 cells randomly in the rectangular area,

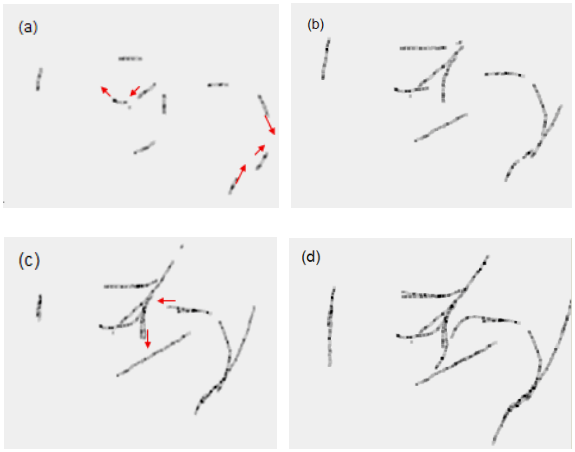

Fig. 7. (a) At 10 time steps, cells have not yet interacted with the slime trails deposited by other cells. The red arrows indicate directions of moving cells (cells are not shown in the figure). (b) At 25 time steps, some cells begin to follow the existing slime trails in the arrow-indicated areas. (c, d) At 40 and 55 time steps, more cells have been following and gliding on slime trails. The cell on the left does not meet any slime trail deposited by other cells, so it keeps gliding and reversing on its own slime trail.

which corresponds to the case of close-packing of cells, because the average area occupied by one cell is 2.5 square-microns, the same as the area of one cell body. The sides a and c in Figure 8 are set to be periodic boundaries, and the upper side of "Initial Area of Cells" acts as a reflecting boundary, that is, when a cell crosses the boundary upwards, it will disappear, while another cell will emerge and cross the boundary downwards. The reason of doing this is that we only simulate a small section of the edge of cell colony, and the cell population in simulation region should keep roughly the same if not considering cell division.

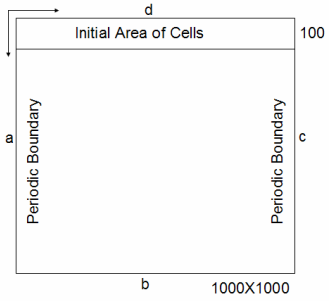

Fig. 8. The simulation region is a 1000×1000 square. Cells are initially distributed in the "Initial Area of Cells" as indicated. Sides a and c are periodic boundaries, while side d acts as a reflecting boundary.

Figure 9 shows the simulation results. We find that the edge solid with cells is broken in some positions, which leads to small gaps. Meanwhile raft and peninsula structures emerge, and the peninsulas are roughly radial if looking at the whole colony circle. These behaviors agree with the experimental observations in Reference [1].

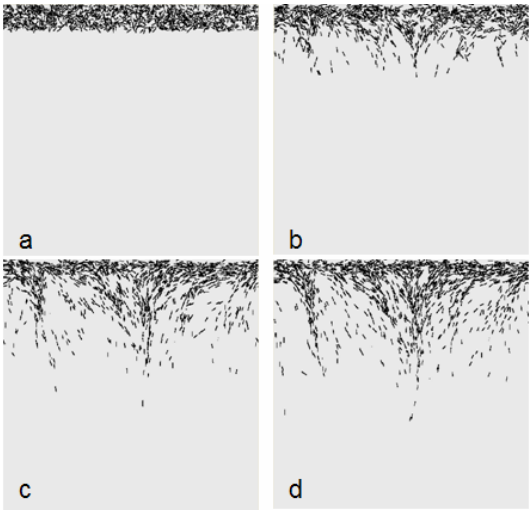

Fig. 9. (a). Initially 1111 cells are randomly distributed in a rectangle area 167 microns in length and 17 microns in width. (b) At 20 minutes, some cells start to move outwards the edge and some small peninsulas form. (c) At 60 minutes and 80 minutes, gaps appear on the initial edge and larger peninsula structures form by merging of smaller ones. The peninsulas point downwards, corresponding to pointing outwards in radial direction if looking at the whole colony circle. The peninsulas are similar to the structures shown in the experimental Figure 1 (END picture).

4 Discussion

Both the modified LGCA model and the off-lattice model presented in this paper can simulate the peninsula formation during Myxobacteria swarming. We have also used modified LGCA model to obtain a quantitative result of the relationship between expansion rate and initial density with the exponential coefficient being within experimental error. However, several artifacts in the LGCA model became apparent while running simulations. The primary one is that a perpendicular direction for peninsula formation only occurred in a few points on the perimeter of the colony. The advantage of this model is that it can model up to tens of thousands of cells, and does produce initial patterns similar to that of experiment.

The off-lattice representation for cells does not have geometric constraints. It allows for bending at small angles and stretching, and incorporates easily a detailed mechanism for slime guidance. Therefore, we expect that the off-lattice model can provide more accurate results for swarming stage. With the off-lattice approach, we

plan to model in detail the quantitative properties of the swarming process, such as the expansion rate and the peninsula dynamics. We are also currently developing parallel algorithms to overcome the computational limitations of this approach.

Acknowledgments. This work was partially supported by NSF Grant No. IBN-0083653 and NIH Grant No. 1R0-GM076692-01: Interagency Opportunities in Multiscale Modeling in Biomedical, Biological and Behavioral Systems NSF 04.6071, and partially supported by US DOE contract number W-7405-ENG-36. Simulations were performed on the Notre Dame Biocomplexity Cluster supported in part by NSF MRI Grant No. DBI-0420980.

References

1. Kaiser, D. and Crosby, C.: Cell movement and its coordination in swarms of Myxococcus xanthus. Cell Motility **3** (1983) 227-245
2. Kaiser, D.: Coupling Cell Movement to Multicellular Development in Myxobacteria. Nature Reviews Microbiology **1** (2003) 45-54
3. Sozinova, O., Jiang, Y., Kaiser, D., Alber, M.: A three-dimensional model of myxobacterial aggregation by contact-mediated interactions. Proc. Natl. Acad. Sci. U.S.A. **102** (2005) 11308-11312
4. Hodgkin, J. & Kaiser, D.: Genetics of gliding motility in M. xanthus (Myxobacterales): two gene systems control movement. Mol. Gen. Genet. **171** (1979) 177-191
5. Wolgemuth, C., Hoiczyk, E, Kaiser, D., Oster G.: How Myxobacteria Glide. Curr. Biol. **12** (2002)369-377
6. Kaiser, D., and Yu, R.: Reversing cell polarity: evidence and hypothesis. Cur. Opin. Microbiol. **8** (2005) 216-221
7. Kaiser, D. Signaling in Myxobacteria. Annu. Rev. Microbiol. **58** (2004) 75-98
8. Burchard, R. P.: Trail following by gliding bacteria. J. Bacteriol. **152** (1982) 495-501
9. Gallegos, A., Mazzag, B., Mogilner, A.: Mathematical analysis of the swarming behavior of myxobacteria. Bulletin of Mathematical Biology (In Print)
10. Hardy, J., Pazzis, O., Pomeau, Y.: Molecular dynamics of a classical lattice gas: Transport properties and time correlation functions. Phys. Rev. A **13** (1976) 1949-1961
11. Palsson, E., Othmer, H. G.: A model for individual and collective cell movement in Dictyostelium discoideum. Proc. Natl. Acad. Sci. USA. **97** (2000) 10448–10453
12. Spormann, A. M., Kaiser, D.: Gliding movements in Myxococcus xanthus. J. Bacteriol. **177** (1995) 5846–5852
13. Newman, T. J.: Modeling Multicellular systems using subcellular elements. Mathematical Biosciences and Engineering **2** (2005) 611-622
14. Newman, M. E. J., Barkema, G. T.: Monte Carlo Methods in Statistical Physics. Clarendon Press, Oxford (1999)